AFRL-AFOSR-JP-TR-2023-0080

Quality Estimation during CFRTP Press Molding by Machine Learning of Condition Monitoring

Miyano, Yasushi
KANAZAWA INSTITUTE OF TECHNOLOGY
7-1 OHGIGAOKA, NONOICHI-MACHI ISHIKAWA-GUN
ISHIKAWA, , 9218501
JP

05/11/2023
Final Technical Report

Air Force Research Laboratory
Air Force Office of Scientific Research
Asian Office of Aerospace Research and Development
Unit 45002, APO AP 96338-5002

REPORT DOCUMENTATION PAGE

PLEASE DO NOT RETURN YOUR FORM TO THE ABOVE ORGANIZATION.

1. REPORT DATE	2. REPORT TYPE	3. DATES COVERED	
20230511	Final	START DATE 20200814	END DATE 20230213

4. TITLE AND SUBTITLE
Quality Estimation during CFRTP Press Molding by Machine Learning of Condition Monitoring

5a. CONTRACT NUMBER	5b. GRANT NUMBER	5c. PROGRAM ELEMENT NUMBER
	FA2386-20-1-4042	
5d. PROJECT NUMBER	**5e. TASK NUMBER**	**5f. WORK UNIT NUMBER**

6. AUTHOR(S)
Yasushi Miyano

7. PERFORMING ORGANIZATION NAME(S) AND ADDRESS(ES)
KANAZAWA INSTITUTE OF TECHNOLOGY
7-1 OHGIGAOKA, NONOICHI-MACHI ISHIKAWA-GUN
ISHIKAWA 9218501
JP

8. PERFORMING ORGANIZATION REPORT NUMBER

9. SPONSORING/MONITORING AGENCY NAME(S) AND ADDRESS(ES)	10. SPONSOR/MONITOR'S ACRONYM(S)	11. SPONSOR/MONITOR'S REPORT NUMBER(S)
AOARD UNIT 45002 APO AP 96338-5002	AFRL/AFOSR IOA	AFRL-AFOSR-JP-TR-2023-0080

12. DISTRIBUTION/AVAILABILITY STATEMENT
A Distribution Unlimited: PB Public Release

13. SUPPLEMENTARY NOTES

14. ABSTRACT
During the two years of this research, PIs developed and demonstrated the innovative technologies in digital manufacturing. More precisely it is possible to measure the dynamically varying the material flow during the press molding by evaluating the apparent viscosity under in-line measurements. They also demonstrated that machine learning can be used to monitor process control state from the estimated viscosity, which was one of the main purposes of this research. The other accomplishment of this research includes the visualization of fiber orientation analysis using a new X-ray phase imaging to predict mechanical properties. Unfortunately, extension to 3D fiber orientation analysis of rib shape could not be achieved. Nevertheless, the results obtained in this project are highly contribute to the process control for composite materials related in digital twin, digital manufacturing, and additive manufacturing.

15. SUBJECT TERMS

16. SECURITY CLASSIFICATION OF:			17. LIMITATION OF ABSTRACT	18. NUMBER OF PAGES
a. REPORT	b. ABSTRACT	c. THIS PAGE		
U	U	U	SAR	29

19a. NAME OF RESPONSIBLE PERSON	19b. PHONE NUMBER *(Include area code)*
FUMIO KOJIMA	315-227-7007

Standard Form 298 (Rev.5/2020)
Prescribed by ANSI Std. Z39.18

Final Report for AOARD Grant FA2386-20-1-4042

"Quality Estimation during CFRTP Press Molding by Machine Learning of Condition Monitoring"

May 11, 2023

Name of Principal Investigators: Yasushi Miyano* (PI) and Takehiro Shirai (Co-PI)**

- * E-mail address : miyano@neptune.kanazawa-it.ac.jp
- Institution : Materials System Research Laboratory, Kanazawa Institute of Technology
- Mailing Address : 3-1 Yatsukaho Hakusan Ishikawa 924-0838, Japan
- Phone : +81-76-274-9263 and +81-76-274-9255
- Fax : +81-76-274-9251
- ** E-mail address : shirai@neptune.kanazawa-it.ac.jp
- Institution : Innovative Composite Material Research and Development Center,
- Kanazawa Institute of Technology
- Mailing Address : 2-2 Yatsukaho Hakusan Ishikawa 924-0838, Japan
- Phone : +81-76-276-3100, Fax : +81-76-276-3101

Period of Performance: 14 Aug 20 to 13 Feburary 22 (Two Years + NCE Six Months)

Abstract

A feature of thermoplastic carbon fiber composite material (CFRTP) is that it has high productivity that enables secondary processing such as press molding. However, there is a problem that the mechanical property of the products is uneven after press molding. The cause is that the resin melted in the press mold flows under the compression load during press molding, and the fiber orientation is different from the original material. The conventional in-process quality checking method only determines whether a measured value of a pressure sensor or the like mounted on a press die exceeds a control value, and cannot predict a material flow during molding. The purpose of this research is to develop a technology that recognizes the time series change of sensor data during press forming as a pattern and determines the quality accompanying the material flow during press forming by machine learning. First, we will develop sensor data patterning technology for viscoelastic changes at each temperature and strain rate during CFRP press molding. Second, we observe the fiber orientation change inside the molded product, and model the material flow state during press molding and evaluate the mechanical properties. Third, machine learning is performed using sensor data patterns and machine characteristic data. As a result, a technology for estimating product quality from sensor data during press molding will be developed.

Introduction

The purpose of this technology development is to develop mass production technology for the CFRP products press molding. Conventional optimization method for CFRP press molding is that press molding is performed after determining the molding conditions such as temperature, press load and speed, the quality of the molded product is determined by the test, and the validity of the molding conditions is evaluated. However, in the conventional method, it is difficult to produce the products of the same quality even if press molding is performed under constant production conditions. The reason is that the carbon fiber laminate structure of the CFRP material being heated expands as the resin melting. Then, the fibers and the resin flow in the mold by the compression load of the press molding, and change into a fiber laminated structure different from the material before the press molding. This is a reason for the variation in the internal structure of the fiber and the resin during the press molding, which causes variations in the quality of the molded product even in the press molding under a constant production condition.

In general, quality control methods during processes such as press molding use pressure and resin temperature sensors mounted on the molding die to measure changes during molding and determine whether the specified pressure and temperature have been reached. However, in this method, since only one point of measurement data is determined, it is not possible to determine a change in the resin state inside the mold during press molding.

Recently, we noticed that the time series data of the die displacement sensor during press molding showed a different pattern for the difference of heating temperature and press load. However, the change in the unique pattern is extremely small and cannot be determined by a human. So, as a result of examining the pattern recognition by machine learning, it was found that the classification can be made under a single condition of the heating temperature and the press load. However, pattern classification is complicated and difficult because actual press forming is a complex condition.

In the maintenance field for example aircraft engines, Digital Twin technology based on sensor measurement is applied. But, in the manufacturing filed, there are various external factors other than manufacturing conditions, so it is difficult to develop Digital Twin technology at the manufacturing filed. Therefore, in this study, instead of pattern classification of sensor time series data during press molding including external factors, actual measurement data of viscoelastic change of CFRP material and material flow state obtained by analysis of fiber orientation change of molded product are combined. Then, pattern classification is performed using sensor time-series data based on the material viscoelastic properties. With this method, it is possible to directly observe the state of material change during molding even when external factors are involved. Then, by using this pattern and machine learning of product mechanical characteristics, we will develop technology for estimating the quality of products in molds from sensor data during press molding.

Objectives

The purpose of this research is to develop FRP press molding mass production technology. We noticed that the time series data of the die displacement sensor during press molding showed different patterns for the difference of heating temperature and press load. Therefore, first, we will develop a sensor data patterning technology for viscoelastic changes at each temperature and strain rate during CFRP press forming. Second, we observe the fiber orientation change inside the molded product, and model the material flow state during press molding and evaluate the mechanical properties. Third, machine learning is performed using sensor data patterns and machine characteristic data. As a result, a technology for estimating product quality from sensor data during press molding will be developed.

Approach

1. Patterning of sensor time series data during press forming

In order to obtain the relationship between viscoelastic properties and material flow due to differences in material temperature and compression speed settings during press molding and compression, an experiment was conducted to acquire physical properties using a compression flat plate tester, and material viscoelasticity and compression load The sensor time series data is measured. In addition, a material compression test was performed with a 2000 kN press molding machine and an experimental mold in which sensors were arranged in an array on the mold surface. Perform patterning.

2. Observation of fiber orientation inside molded products and development of mechanical property prediction technology

Observe the fiber orientation inside the molded product by X-ray CT image analysis of CFRP molded product, and analyze the change in fiber orientation due to material flow.

Since an X-ray CT image has a trade-off relationship between the observation range and the resolution, the observation range is as small as about several mm in order to obtain detailed fiber orientation analysis information, and the entire molded article cannot be observed. Therefore, in order to obtain the fiber orientation information of the entire molded product, it is necessary to obtain the fiber orientation information that has been homogenized within a certain range, and it is necessary to optimize the element size when simulating the mechanical properties. In this section, we will develop a technique for analyzing fiber orientations with an observation range of several hundred mm using phase imaging technology, a new X-ray observation technique. Then, the consistency between the mechanical property values obtained from the actual test, the mechanical properties predicted from the fiber orientation results, and the fracture model is examined.

3. Development of Judgment Technology for Press Forming Using Machine Learning

Machine learning is performed by combining the sensor time series pattern of 1 with the fiber orientation and mechanical property results of 2, and a technology to predict the mechanical properties from the sensor time series data during press forming is developed.

Machine learning models are customized based on readily available existing models.

Then, using the constructed machine learning model, the time series data of the actual press forming sensor is analyzed, the validity of the learning model is evaluated, necessary improvements are made, and the proof is confirmed.

1. Patterning of sensor time series data during press forming

1.1 Introduction

Chopped carbon fiber tape-reinforced thermoplastic (CTT) has high strength and formability, and is attracting attention as a next-generation composite material. Figure 1-1 shows the structure and photograph of the CTT press-formed flat plate. Carbon fiber tape pieces of several tens of millimeters in length impregnated with thermoplastic resin are laminated in random directions and press-molded. Figure 1-2 shows the CTT manufacturing process. Because the carbon fibers in this material are discontinuous, the material melted in the mold flows during press molding, enabling complex product shapes with ribs to be produced in a single press molding. CFRP material during press molding undergoes biaxial flow due to compressive load. Rheometers typically measure the viscosity of polymeric materials. However, CTT exhibits anisotropic flow properties because it flows significantly in the transverse direction of the fiber orientation [1]. And due to the strong influence of the fiber structure, rheometers cannot give accurate measurements. Therefore, we used a universal material testing machine to increase the size of the test piece to reduce the variation in the measurement of CFRP viscosity. First, using a universal material testing machine equipped with a high-temperature chamber, we obtained measurement data on the strain rate dependence and temperature dependence of the apparent viscosity of the molten CFRP material. This data was used as master data. Apparent viscosities were then calculated by combining sensor readings from press molding experiments. Since the apparent viscosity measured in the press molding experiment and the apparent viscosity of the master data matched, it was proved that the apparent viscosity of the CFRP material measured by the press molding machine is a reasonable value.

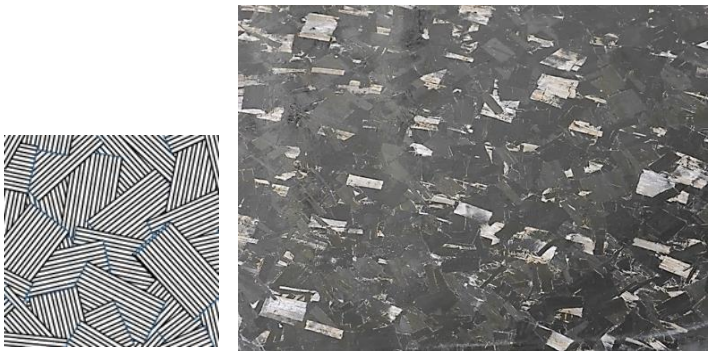

Fig. 1-1 Structure and photograph of a press-molded flat plate of CTT

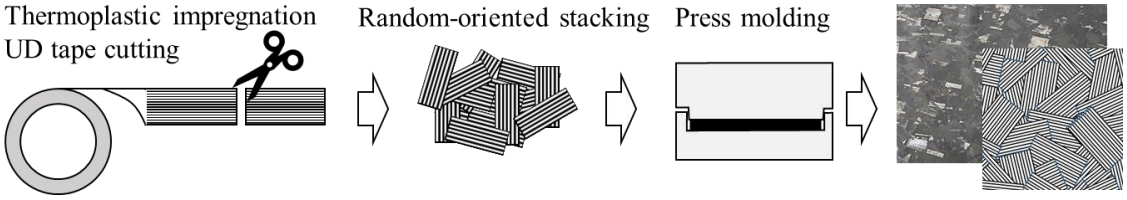

Fig. 1-2 The CTT manufacturing process.

1.2 Measurement of apparent viscosity with a universal tester

Figure 1-3 shows the arrangement of the compression flat plate test jig and test specimen in the constant high-temperature chamber. The specimen was a disk shape with a diameter (D) of 75 mm and a thickness (H_0) of 6 mm. The compression flat plate jig's moving speed was 0.01, 0.1, 1, 10 mm/sec under four conditions, and the material heating temperature was 200, 175, 150, 125 °C under four conditions. The test piece was assumed to be an incompressible material, and the Poisson's ratio was 0.5. The compressive pressure σ when flowing in the x-direction due to the load in the y-direction was calculated by Eq. (1), the strain ε was calculated by Eq. (2), and the strain rate $\dot{\varepsilon}$ was calculated by Eq. (3). The test load was F, and the test piece thickness H was the distance between the compression plate jigs. In this study, we calculated the apparent viscosity because it was difficult to formulate the viscosity change of non-Newtonian fluid during the molding process. The apparent viscosity was calculated by Eq. (4) from the changes in pressure and strain rate [4].

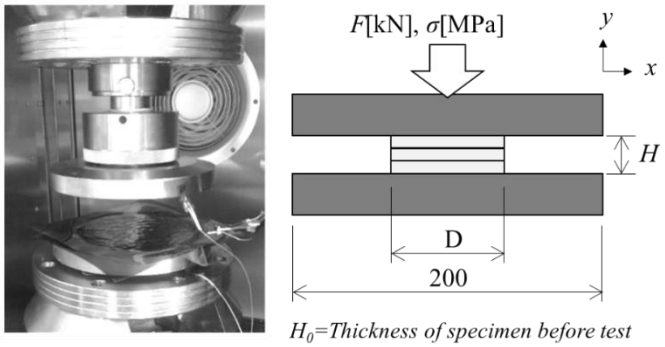

Fig. 1-3 Specimen compression test method for universal material tester (Left Figure: Photograph of compression test flat plate jig and specimen arrangement, Right Figure: Outline view of compression test)

$$\sigma[MPa] = \frac{4}{\pi}\frac{F}{D^2}\frac{H}{H_0} \quad (1)$$

$$\varepsilon = \ln\left(\frac{H}{H_0}\right) \quad (2)$$

$$\dot{\varepsilon}[1/sec] = \frac{1}{H}\frac{dH}{dt} \quad (3)$$

$$\eta_{ap}[MPa.sec] = \frac{\sigma}{\dot{\epsilon}} \quad (4)$$

Figure 1-4 shows the results of compressive stress change during the test. The horizontal axis is the position of the compression plate and the plate jig position where the upper and lower plate jigs contact is set to 0 mm. The vertical axis is the compressive stress value calculated by equation (1). Each graph shows the test temperature of 200 degrees and the results of four test speed conditions. Figure 1-5 shows the results of strain rate change during the test. The vertical axis is the strain rate calculated by equation (3). Figures 1-4 and 1-5 alone cannot accurately observe the material flow under compressive load.

Figure 1-6 shows the result of the apparent viscosity change during the test. The vertical axis shows the apparent viscosity calculated by Eq. (4), and each line in the Figure shows the test result of one test piece. Figure 1-7 shows that the change in apparent viscosity in the range of 5 to 3 mm at the flat plate jig position where the test piece is flowing due to the compressive load shows the same slope at each test speed. The 175, 150, and 125 ° C material heating temperatures also have the same trend. Figure 1-7 shows the strain rate dependence results of the apparent viscosity of the CTT material. The value at the compressed plate position 5 mm, where the material flow starts in Figure 1-6, is plotted for the apparent viscosity value. Heating temperatures 175, 150, and 125 ° C were also plotted in the same way. The apparent viscosity changes linearly to the strain rate, and the material viscosity during molding changes depending on the die speed during press molding. In addition, the smaller the material heating temperature, the greater the change in apparent viscosity, showing a temperature dependence. Figure 1-7 was used as the CTT material flow database for this experiment and compared with the press molding experiment results.

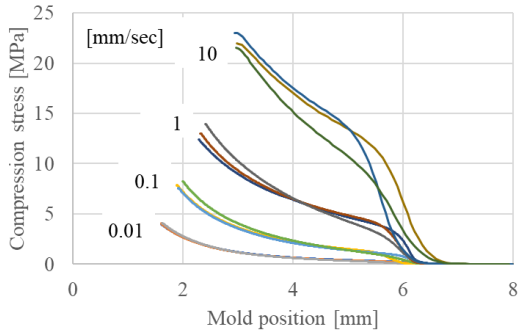

Fig. 1-4 Results of compression stress measurement (material temperature 200 °C, mold speed 0.01, 0.1, 1, 10 mm / sec)

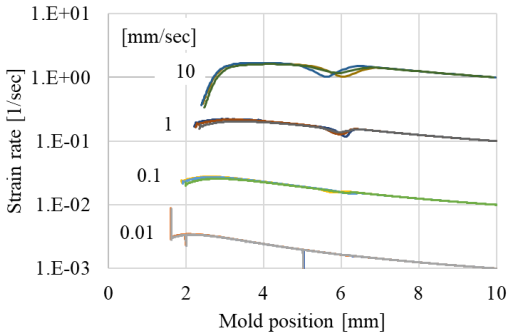

Fig. 1-5 Results of strain rate measurement (material temperature 200 °C, mold speed 0.01, 0.1, 1, 10 mm / sec)

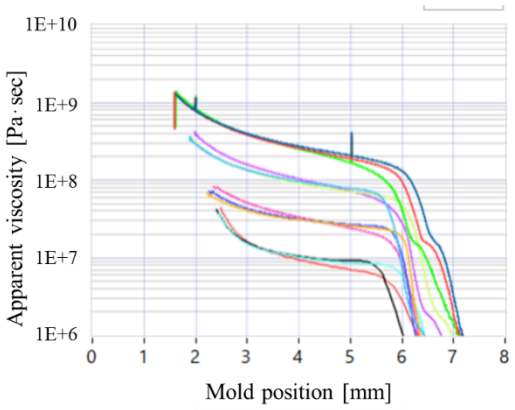

Fig. 1-6 Results of apparent viscosity measurement (material temperature 200 °C, mold speed 0.01, 0.1, 1, 10 mm / sec)

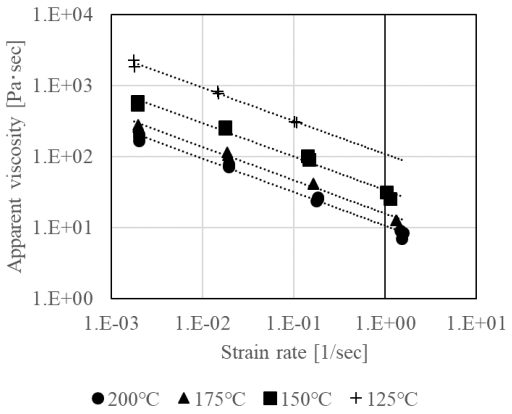

Fig. 1-7 Results of CTT's apparent viscosity dependence on strain rate (material temperatures 200, 175, 150, 125 ° C)

1.2 Measurement of apparent viscosity with a 2000 k N hydraulic press machine

Figure 1-8 shows the schematics and dimensions of the molded product used in the experiment. A pressure sensor (6157BA, KISTLER) was installed in the molding die, and we measured the pressure in the outer center of the convex shape of the molded product in the black circle ● part. CTT material was 200 x 80 mm, the thickness was 8mm and put into the center of the press molding die. Table 1-1 shows the seven press molding conditions tested. The press molding conditions were that the mold and material temperatures were kept at 200 °C for 3 minutes and then cooled to 80 °C.

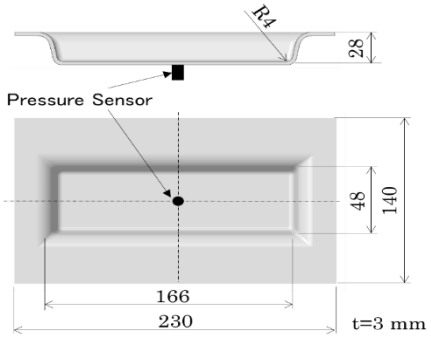

Fig. 1-8 Drawing showing the molded product of the press molding experiment and the measurement position of the pressure sensor

Table 1-1 Seven conditions for press molding

Sample	Temperature [°C]	Speed [mm/sec]
A	200	10
B	200	10
C	200	1
D	200	1
E	150	10
F	150	1
G	150	1

experiments

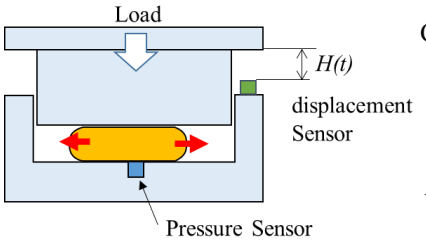

Compressive stress $\sigma[MPa]$ = Value of pressure sensor in mold

Strain rate $\dot{\varepsilon}[1/sec] = \frac{1}{H}\frac{dH(t)}{dt}$ (5)

Apparent viscosity $\eta_{ap}[Pa \cdot s] = \frac{\sigma}{\dot{\varepsilon}}$ (6)

1.3 Result and discuss

Figure 1-9 shows the results of compressive stress change during the test, and Figure 1-10 shows the results of strain rate change. The compression pressure σ is the measured value of the resin pressure sensor mounted on the mold, and the specimen thickness H is the measured value of the laser displacement sensor installed on the mold. Figure 1-11 shows the results of the apparent viscosity. The apparent viscosity of the material in the mold during press molding was calculated by Eq. (4). The apparent viscosity changes gently in the 8 to 4 mm region where the material was flowing in the mold. Therefore, we inferred that it is in a continuous flow state.

Figure 1-12 shows the result of adding the apparent viscosity of the press molding experiment to Figure 1-7 of the strain rate dependence of the apparent viscosity measured by the universal material tester. The results for the seven press molding conditions in Table 1 are white plots, added to the 200 ° C and 150 ° C results in Figure 1-7. The apparent viscosity of the press molding experiment is the value at the mold position 8 mm, where the material flow starts. The apparent viscosity values in the press molding experiments agreed with the apparent viscosity values in the database created by measuring with a universal material testing machine. Thus, the results showed that the material flow in the mold during press molding, which was not possible until now, can be directly measured by the apparent viscosity.

The apparent viscosity measurement method obtained in this section is a value that accurately measures

the flow of material during press molding. Therefore, the time variation of the apparent viscosity will greatly contribute to the pattern analysis of machine learning. Next fiscal year, we plan to conduct press molding experiments with various fiber structures and molding conditions to obtain the apparent viscosity.

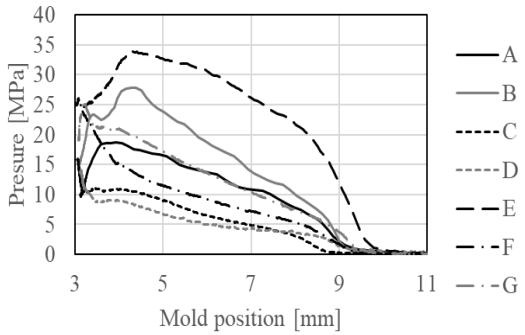

Fig. 1-9 Results of pressure measurement in press molding experiments

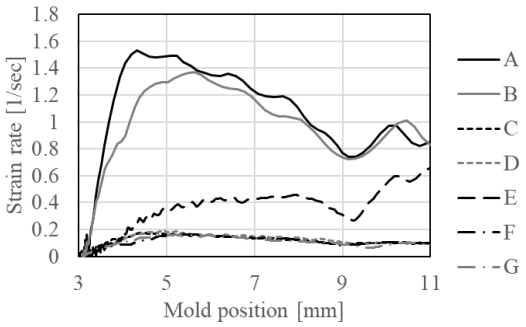

Fig. 1-10 Results of strain rate measurement in press molding experiments

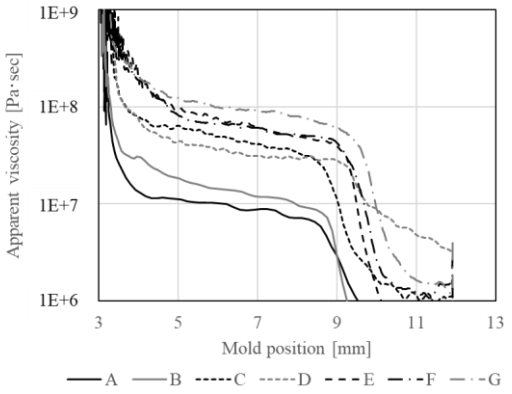

Fig. 1-11 Results of apparent viscosity measurement in press molding experiments

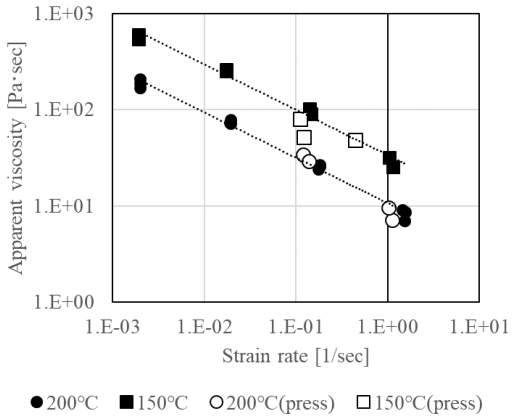

Fig. 1-12 The result of adding the apparent viscosity measurement result of the press molding experiment to Fig. 4. (the black plot is the result of the universal material tester, the white plot is the result of the press experiment.)

2. Observation of fiber orientation inside molded products and development of mechanical property prediction technology

2.1 Introduction

In chopped carbon fiber tape reinforced thermoplastic (CTT) material, the anisotropic region of fiber orientation after press molding often causes the degradation of mechanical properties and damage and fracture. This study explores means of obtaining the fiber shape and fiber orientation tensors from molded products and then predicting the CTT mechanical properties and damage fracture locations.

The fiber orientation tensor of the molded product was obtained through X-ray phase imaging. The material properties of the finite element model using CTT were calculated and mapped from the fiber waviness model and the orientation tensor to predict damage failure. Results showed that the fracture positions of both the test and simulation agreed in specimens having large anisotropic regions. However, the specimens with small anisotropic regions did not match. Therefore, the images of strain distribution of the test piece under a tensile load were compared by cross-correlation. Results showed a large correlation between the tensile test and simulation results, thus confirming the simulation's effectiveness.

2.2 X-ray CT imaging of CTT molded products

Figure 2-1 shows the results of the fiber shape obtained by X-ray CT image and image processing. The test pieces are a prepress test piece with laminated tape and a test piece after press molding. We found that the fiber shape waviness greatly due to the flow of the material during press molding. So, in the damage fracture simulation, We calculated the material properties considering the fiber waviness.

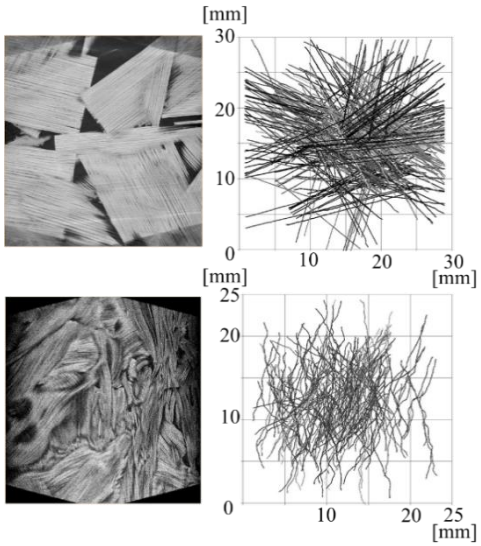

Fig. 2-1 Results of X-ray CT image and image-processed fiber shape of CTT tape-laminated pre-molded test piece and post-press-molded test piece (a, b: X-ray CT image, c, d: Fiber shape of image processing result, a, c: Specimen of before press molding, b, d: Specimen of after press molding.)

2.3 X-ray phase imaging of CTT molded products and acquisition of fiber orientation tensor

X-ray phase imaging is an imaging technique for detecting a phase shift of X-rays when passing through a subject. Figure 2-2 shows the principle of the X-ray phase imaging device. The X-ray Talbot Low Interferometer is one of the X-ray phase imaging methods. First, the fiber orientation of the CTT specimen was obtained from the image analysis using an X-ray phase imaging device (Shimadzu Corporation) [6]. Next, and we calculated the 2D fiber orientation tensor from the fiber orientation [7,8,9].

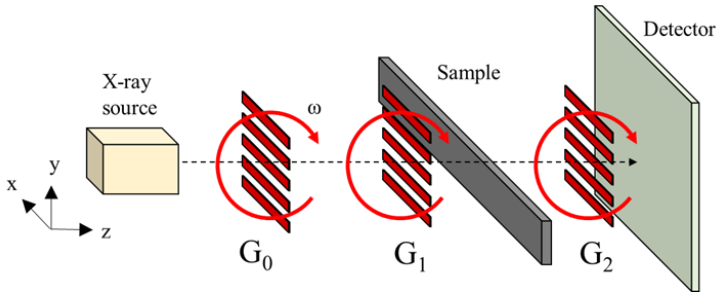

Fig. 2-2 Schematics of X-ray Imaging System. Transmission gratings (G0, G1, and G2) are placed in-line along the beam

2.4 Creation of damage fracture model using fiber orientation tensor.

We used GENOA (Alpha Star, USA) for the damage fracture prediction simulation [9, 10, 11]. First, the GENOA inhomogeneation method calculation creates the single-layer composite model. Table 2-1 shows the calculation results of the mechanical properties of the single-layer composite model. Tables 2-2 and 2-3 show the material properties and structural design used in the calculations. Next, the fiber orientation tensors were mapped for each FEM model element. Then, multiple single-layer composite models are stacked for each FEM model element and calculate the material properties according to the fiber orientation tensor.

Table 2-1 Results of mechanical properties of single-layer composite model obtained by calculation

Property	
Longitudinal Modulus E_{11} [GPa]	48.5
Transverse Modulus E_{22} [GPa]	5.0
Shear Modulus G_{12} [GPa]	4.3
Tensile Strength S_{11T} [MPa]	377.1
Compressive Strength S_{11C} [MPa]	314.9
Tensile Strength S_{22T} [MPa]	39.2
Compressive Strength S_{22C} [MPa]	39.2
Shear Strength S_{12} [MPa]	38.8
Poisson's ratio v_{12}	0.37

Table 2-2 Mechanical properties of fibers and resins used in the calculation of the single layer composite

	Fiber	Matrix
Density [g/cm^3]	1.98	1.18
Modulus [GPa]	240	2.4
Poisson's ratio	0.21	0.3
Tensile Strength [MPa]	4,148	59
Compressive Strength [MPa]	2,532	59
Shear Strength [MPa]	-	35

Table 2-3 Fiber structure and lamination conditions used in the calculation of the single-layer composite

Property	
Fiber length [mm]	26
Fiber diameter [㎛]	7
Fiber volume ratio [%]	40
Void volume ratio [%]	0.1
Fiber waviness length [mm]	13
Fiber waviness amplitude [mm]	0.5
Total thickness [mm]	2
Number of layer	1
Material type	Aligned

Figure 2-3 shows the color vector map, the fiber orientation tensors, and the material properties. a) is the orientation angle distribution by the color-coded circle color for each angle, and the shade of the image shows the degree of orientation. The bright part of the shade image shows the unidirectional fiber orientation part with large anisotropy, and the dark part shows the isotropic random orientation. a) is a structure in which the fiber orientation is not uniform and random, but local fiber orientation bias and anisotropic structure are distributed. b, c, d) are the results showing the values of the orientation tensors A11, A22, and A12 calculated from a) on a color scale. e) is the material property mapping result for each element calculated by GENOA from the orientation tensor, and 21 different material properties are color-coded and defined.

2.5 Damage fracture simulation results with fiber orientation tensor

Fracture damage analysis was calculated with the PFA module of GENOA [12]. Figure 2-4 shows the results of the damage fracture simulation of 6 test pieces. a) is the fiber orientation distribution color vector map acquired by the phase imaging device. b) is a photograph of the fracture of the test piece after the tensile test. c) is the result of the damage fracture simulation. Blue indicates the healthy part, red indicates

the part where the damage fracture occurred, and the white outline indicates the fractured part where the element is missing due to the fracture. d) is the strain distribution result immediately before fracture in the tensile direction X by DIC analysis during the tensile test. e) is the result of the strain distribution just before the fracture in the X direction by simulation. The results of Specimen Nos. 5, 3, and 2 shows that the fracture position of the tensile test and the simulation fracture position is the same in the anisotropic region (light blue part), where the fiber orientation distribution was orthogonal to the tensile direction X. This result shows that the damage fracture simulation using the fiber orientation tensor obtained from the test piece shows good agreement with the actual tensile test results. Thus, it is possible to predict the damage fracture of the molded product with high accuracy. Next, the results of Nos. 6, 1, and 4 show that there are no large regions showing anisotropy, and small areas are scattered compared to Nos. 5, 3, and 2. The fracture position of the tensile test and the simulated fracture position were different results.

The intercorrelation coefficients of the strain distribution images of d) and e) of the six samples were calculated to verify the validity of the simulation. Figure 2-5 shows the results of the intercorrelation coefficient. Since the result of Figure 2-5 has a correlation coefficient of 0.4 or more, the correlation between the strain distribution at the tensile test and the strain distribution of the simulation result is shown. Thus, from the correlation coefficient results, the simulation results appropriately predicted changes in the strain of the test piece, and We found the validity of the simulation results.

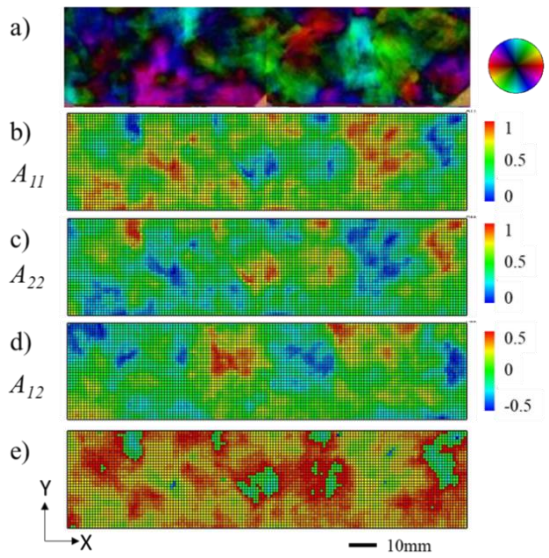

Fig. 2-3 Results of fiber orientation tensors and material properties defined for each simulation element.
(a: Color vector map of fiber orientation obtained by phase imaging, b, c, d: Color map of fiber orientation tensor A11, A22, A12)

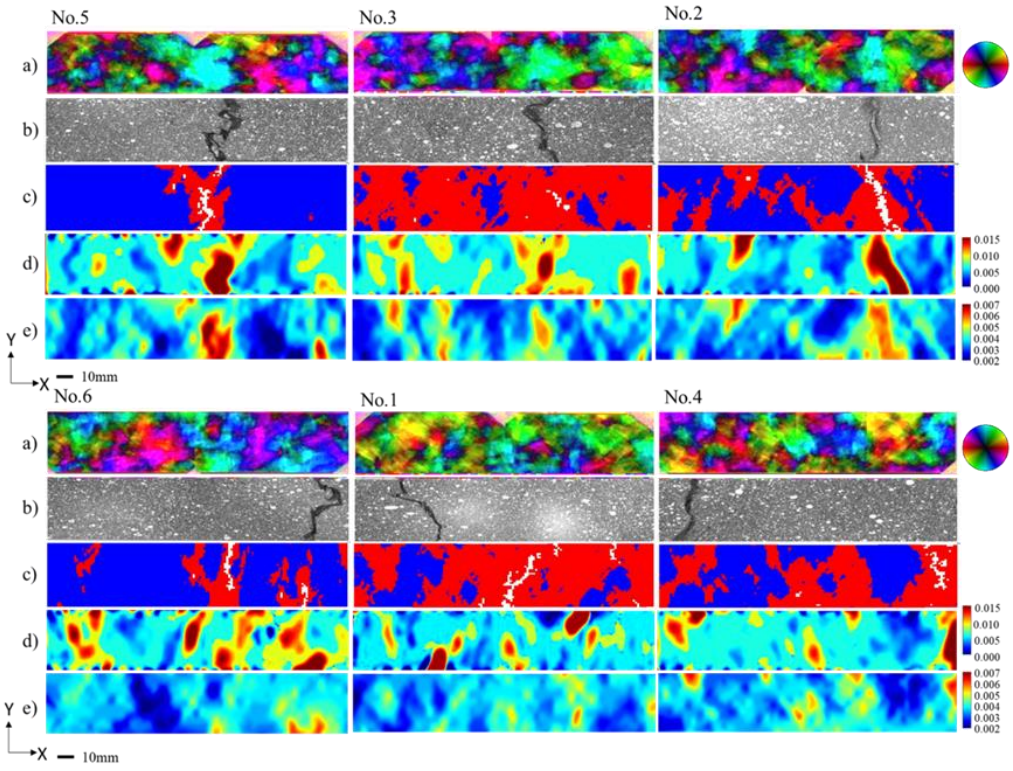

Fig. 2-4 Results of phase imaging images, tensile test and damage fracture prediction simulation for each test specimen. a) Color vector map of fiber orientation and degree of orientation, b) Photograph of specimen fracture after tensile test, c) Results of damage fracture simulation, d) Color map of strain distribution of DIC analysis results during tensile test, e) Color map of strain distribution of damage fracture simulation results.

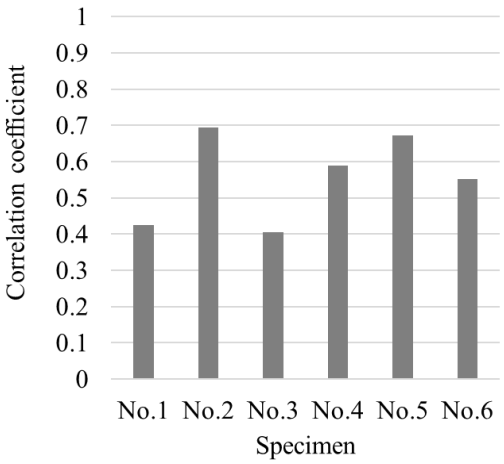

Fig. 2-5 The results of calculation of cross-correlation of in-plane strain distribution color map images of tensile test and damage fracture simulation.

3. Development of Judgment Technology for Press Forming Using Machine Learning

3.1 Introduction

The application of machine learning techniques in manufacturing has become increasingly popular in recent years [13.14]. The use of machine learning in manufacturing has the potential to significantly improve efficiency, reduce costs, and enhance product quality. In recent years, research has been conducted on advancing carbon fiber reinforced plastics (CFRP) manufacturing using machine learning techniques. One of the main goals of this research is to optimize the manufacturing process of CFRP through the application of machine learning algorithms. For example, machine learning models can be trained on data obtained from the manufacturing process to predict the optimal processing conditions for achieving high-quality CFRP products. Another aspect of this research is the use of machine learning for real-time monitoring and control of the CFRP manufacturing process. This involves the integration of sensors and other data collection devices with machine learning algorithms to enable continuous monitoring and adjustment of the manufacturing process based on real-time feedback. The application of machine learning to CFRP manufacturing has the potential to enhance the quality and efficiency of the manufacturing process significantly. By optimizing the process and improving real-time monitoring and control, it is possible to reduce waste and improve the consistency and reliability of the final product.

In this chapter, we used the apparent viscosity measurement method of the press forming obtained in Chapter 1 to determine the flow state of the material in the mold during forming using machine learning from the sensor measurement data during press forming. At the beginning of the research, we aimed to estimate the mechanical properties of the press mold product by integrating the fiber orientation analysis results in Chapter 2. However, it was very difficult to consider it, and I reluctantly gave up.

3.2 Creation of apparent viscosity data for machine learning

The acquisition of press molding data for judging different molding conditions by machine learning was investigated. From Chapter 1, the apparent viscosity calculated from the data measured by the pressure sensor and the displacement sensor mounted on the mold reflects the material flow inside the mold well. Since the apparent viscosity depends on the temperature of the material and the mold, it is possible to determine the temperature change of the molding conditions by the magnitude of the apparent viscosity. Also, the mold speed is the same because it can be determined whether the time response is fast or slow. Therefore, we took on the challenge of using machine learning to determine differences in the material flow inside the mold, which is difficult to determine.

Figure 3-1 shows the shape of the two molded products used in the experiment. The shapes of the molded product were the same as the experiment in Chapter 1, but we used two types, rib and ribless, in the hollow part. The ribless molded products have a shape that simulates the defective state of short-shot molding defect in which

the material flow does not reach the ribs. If the two molded shapes were recognized by machine learning, rib and ribless, it would be possible to judge the defective molding condition from measurement sensor data during the press molding process. The apparent viscosity during press molding was measured using these two products. The molding conditions were the fixed conditions shown below.

- Material: Matrix thermoplastic epoxy (same CTT material as in Chapter 1)
- Material heating, mold temperature: 200℃
- Mold speed: 10 mm/sec

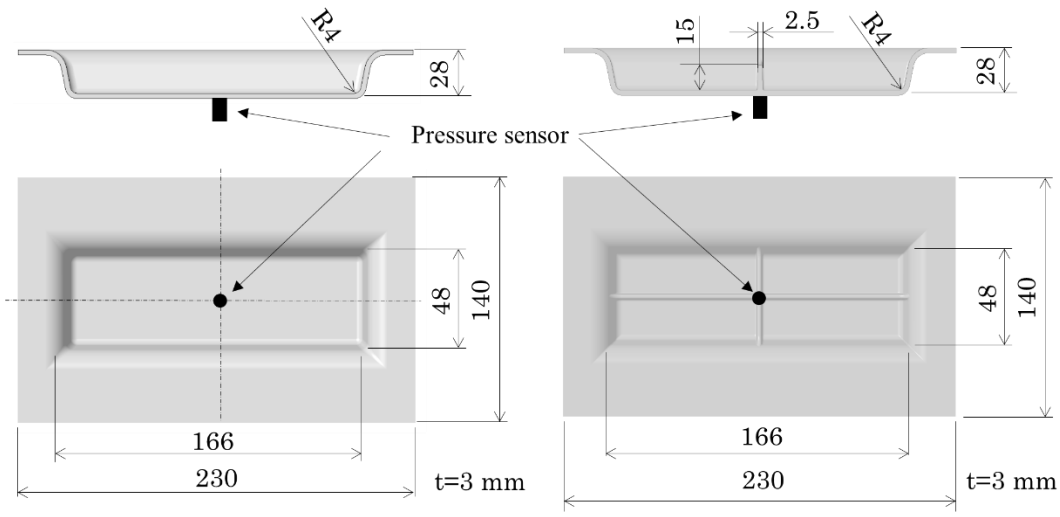

Fig. 3-1 The schematics of the two molded products used in the experiment
(Left Figure: ribs product. Right Figure: ribless product)

Figure 3-2 shows the measurement results of apparent viscosity. The horizontal axis is the position of the upper mold relative to the lower mold, and the vertical axis is the value of the apparent viscosity. These results include data for moldings rib and ribless. Since the pressure sensor and displacement sensor data were acquired at intervals of 0.2 sec, the mold position on the horizontal axis was not acquired at equal intervals. For machine learning to recognize data, response intervals, such as the time and position of each data, must be the same. Therefore, we processed the data so that the horizontal axis data of all the results in Figure 3-2 were evenly same interval. Figure 3-3 shows the processing method. Small fluctuations accompany apparent viscosity data due to variations in sensor measurement data, which is an obstacle for machine learning. Therefore, we approximated the apparent viscosity data with a ninth-order polynomial. The blue dot plot graph in Figure 3-3 results from apparent viscosity calculated from sensor measurement data (measure), and the green graph (fitting) is the result of approximation with a 9th-order polynomial. A ninth-order polynomial was then used to calculate the apparent viscosity at 0.1 mm intervals between mold positions. The results are shown in a red dot graph (Resample). Figure 3-4 shows the processed result. a)

is the apparent viscosity data from the mold position 5mm where the apparent viscosity showed a constant value in the material flow in Fig. 3-2, b) is the result of approximation with a 9th order polynomial, c) is the metal viscosity from the 9th order polynomial This is the result of recalculating the apparent viscosity at intervals of 0.1 mm for the mold position.

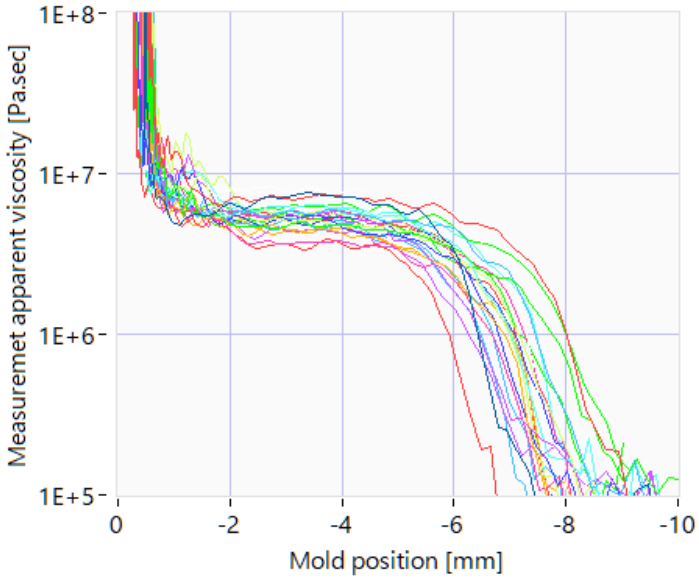

Fig. 3-2 The result of measurement apparent viscosity during press molding.
(24 data in total, 19 data for rib molded products, 5 data for ribless molded products)

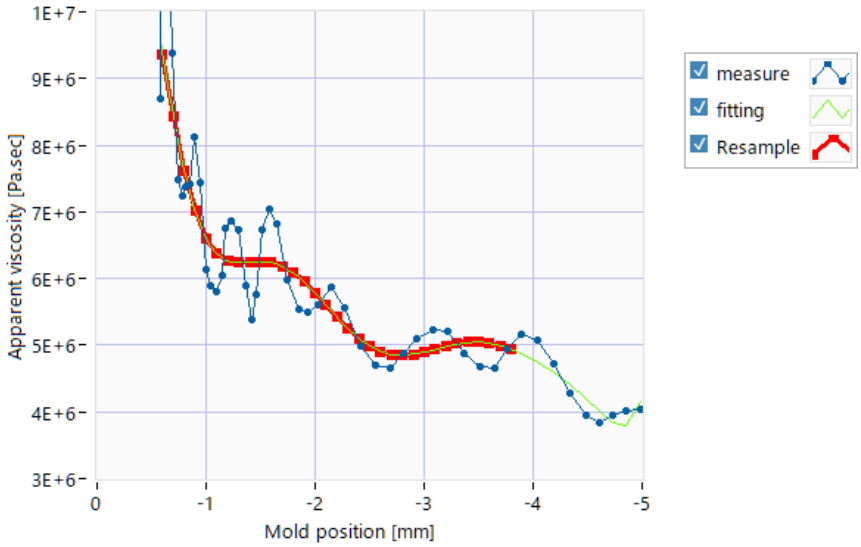

Fig. 3-3 The result of processing apparent viscosity data at equally spaced mold positions

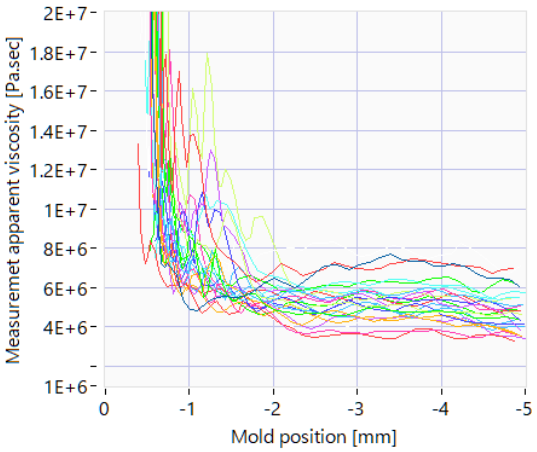

a) Apparent viscosity data from mold position 5mm in Figure 3-2,

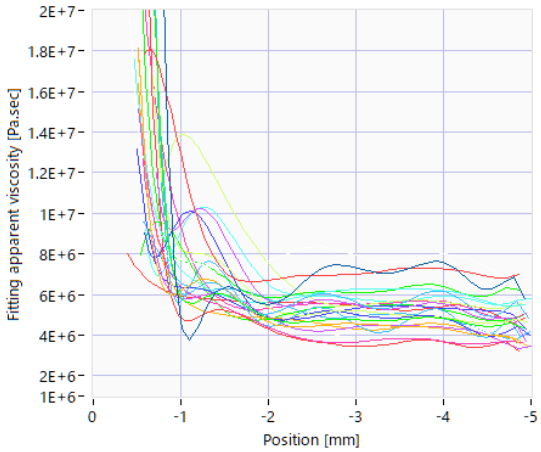

b) The result of the 9th-degree polynomial approximation,

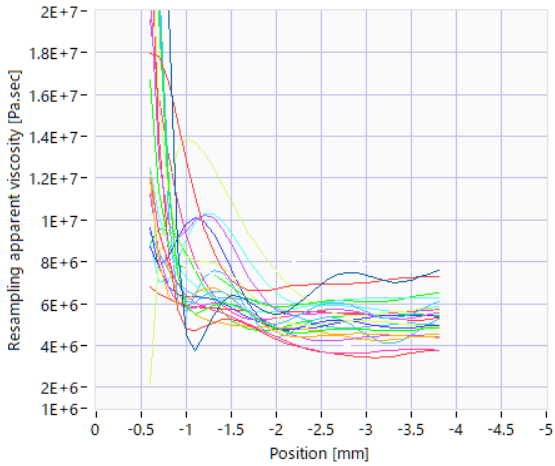

c) Apparent viscosity results calculated from a 9th-order polynomial at 0.1 mm intervals between mold positions

Fig. 3-4 The results of processed apparent viscosity data for machine learning

Figures 3-5 and 3-6 show the results of resampling the apparent viscosity at the mold position at 0.1 mm intervals. Figure 3-5 shows 19 results with cross ribs, and Figure 3-6 show five results ribless. Comparing the two results, it is difficult to determine if there is a visual difference visually.

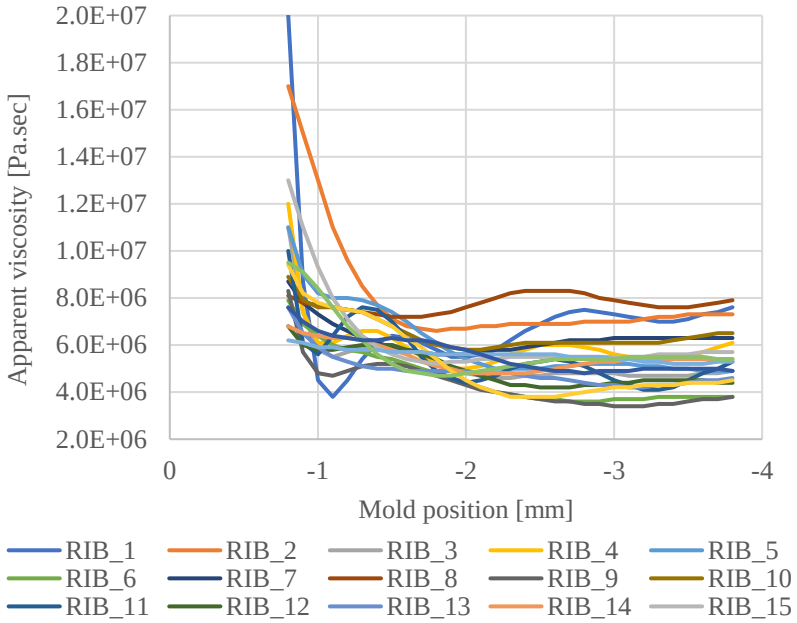

Fig. 3-5 The result of rib molded product resampling the apparent viscosity at the mold position at 0.1 mm intervals

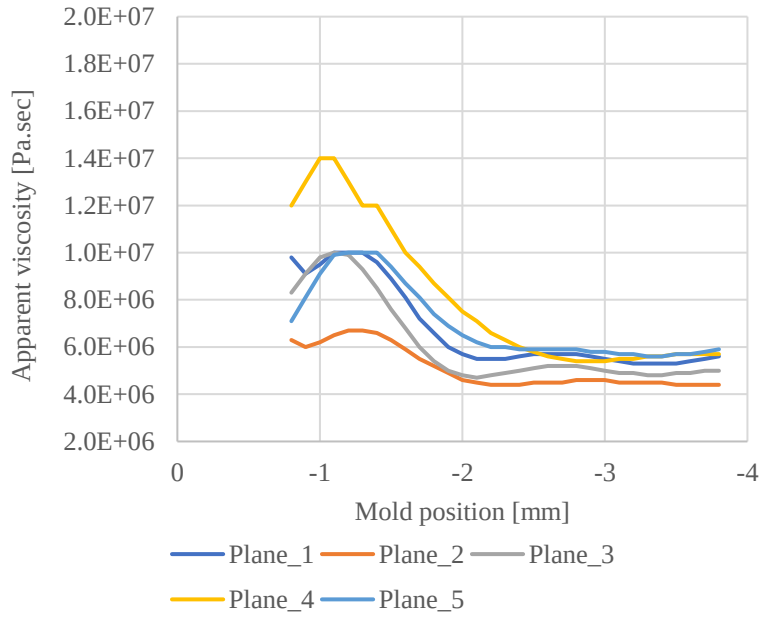

Fig. 3-6 The result of ribless molded product resampling the apparent viscosity at the mold position at 0.1 mm intervals

3.3 Estimation of molding state from apparent viscosity data by machine learning

Apparent viscosity determination by machine learning used MATLAB application. The method is “Fit Data with a Shallow Neural Network”. The description of Fit Data with a Shallow Neural Network shows below from MALTAB help etc.

> Fitting data with a shallow neural network involves training the network to learn the relationship between the input data and the corresponding output data. The shallow neural network consists of an input layer, a single hidden layer, and an output layer. The input layer takes the input data, the hidden layer performs some computation, and the output layer produces the output data.
>
> To fit data with a shallow neural network, we first need to define the architecture of the network, including the number of nodes in the input layer, the number of nodes in the hidden layer, and the number of nodes in the output layer. Once we have defined the architecture, we can train the network using an algorithm such as backpropagation to adjust the weights between the nodes in the network so that the output produced by the network closely matches the desired output.
>
> The process of fitting data with a shallow neural network involves iteratively adjusting the weights in the network based on the error between the actual output and the desired output. This process continues until the error is minimized and the network has learned to predict the output based on the input data accurately.

The network was created using the MATLAB application. Figure 3-7 shows the MATLAB network sample Fit Data with a Shallow Neural Network application. The network is a two-layer feedforward network with a sigmoid transfer function in the hidden layer and a linear transfer function in the output layer. The Layer size value defines the number of hidden neurons. In this study, the hidden layer was 10,

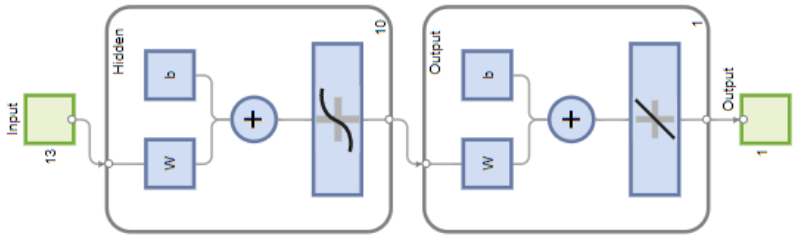

Fig. 3-7 The MATLAB network sample Fit Data with a Shallow Neural Network application.
(Figure source: MATLAB Help Center “Fit Data with a Shallow Neural Network”)

The method by which machine learning determines the apparent viscosity was to create a machine learning data set by associating the apparent viscosity data of a ribless mold, assuming the short-shot molding defect, with the data of correctly molded products with ribs.

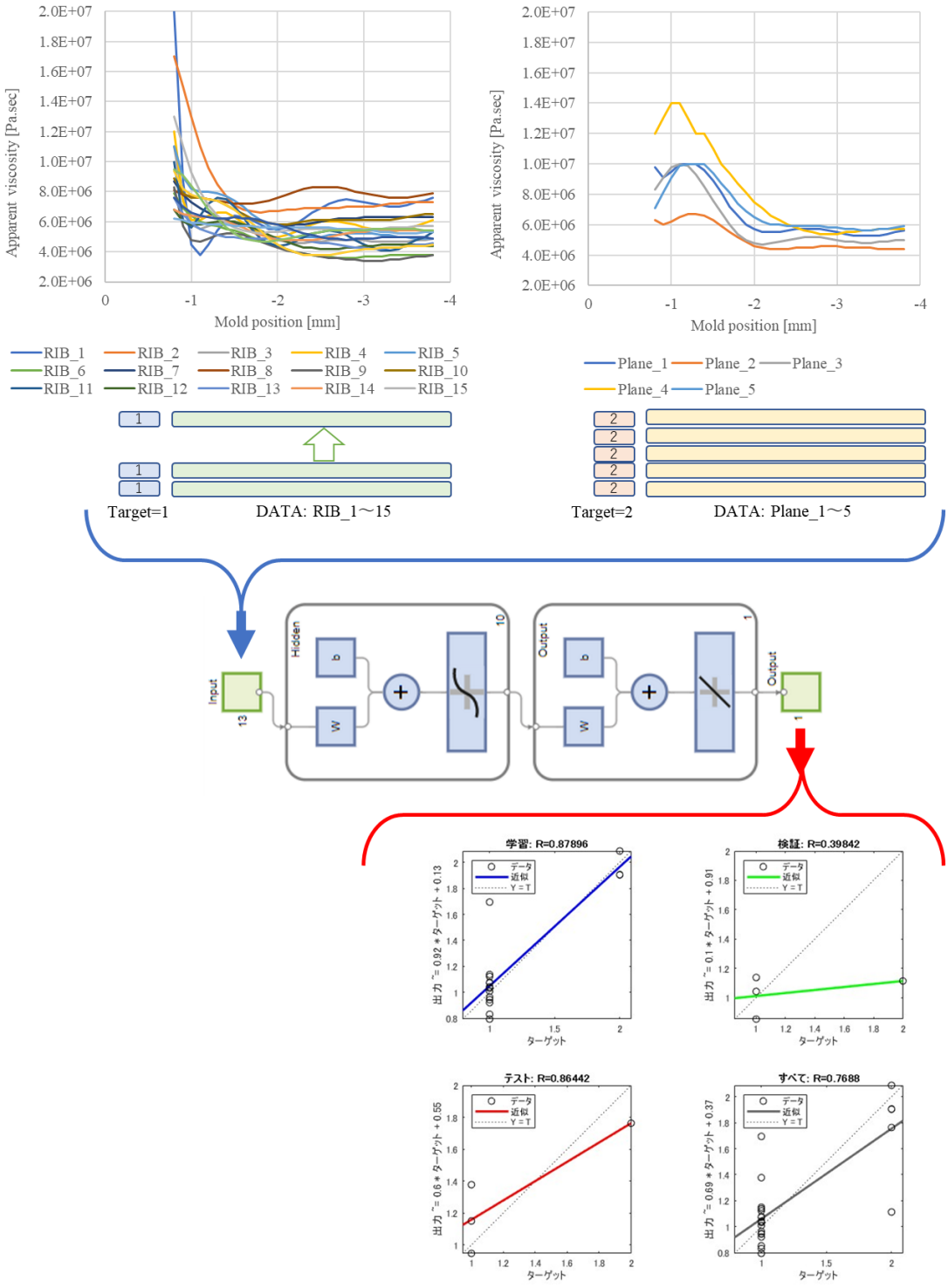

Fig. 3-8 the machine learning method for recognizing apparent viscosity data using a MATLAB application.

Figure 3-8 shows the machine learning method for recognizing apparent viscosity data using a MATLAB application. Apparent viscosity data for molded products with ribs and ribless are in data array (DATA) format with one line each. A machine learning dataset was constructed by linking Target to the data array. The target for molded products with ribs was set to "1", and the target for those ribless was set to "2". Machine learning recognized these data sets and evaluated each data's recognition accuracy.

Machine learning is teaching machines to learn from data without being explicitly programmed. Training, validation, and testing are three critical stages used in this process. The training phase involves feeding the machine learning algorithm with a dataset to help it learn the patterns and relationships between input features and output labels. During this process, the model is optimized by adjusting its parameters to minimize the difference between the predicted and actual outputs. Once the model is trained, it is evaluated on a separate validation dataset. The validation phase aims to estimate how well the model will perform on unseen data. Finally, once the model is tuned and optimized, it is tested on a third dataset called the test dataset. In this study, MATLAB application training algorithm was Levenberg-Marquardt, and Performance was a mean squared error.

Figure 3-9 shows the results of each training, validation, and test phase shown in plots. The horizontal axis of the plot shows the target, and the vertical axis shows the calculated output of each phase. If all the entered apparent viscosity data was recognized as linked Target value, the slope of the plot will show 45 degrees, and the R-value, which indicates the error, will be 1. In other words, when R=1, entered apparent viscosity data of rib molded products were recognized by Target 1, and entered apparent viscosity data of ribless molded products were recognized by Target 2. increase. It shows that data recognition accuracy decreases as the value of R decreases from <1

Machine learning randomly selects data to compute, train, validate, and test from an input dataset. In this study, there were 24 data, and 70% for training, 15% for validation, and 15% for testing were selected. In order to compare the results calculated by selecting different data for each training, we performed training five times. Figures 3-10 to 3-15 show the results of five times of learning. And Table 3-1 shows the error R values resulting from Figures 3-10 to 3-15.

As a result of five calculations, although there were some deviations in learning, verification, and testing, they generally showed a linear slope of 45 degrees, and the average R-value was 0.8 or more. This result indicates that machine learning could recognize the apparent viscosity data during press molding of molded products with ribs and ribless. Therefore, it was shown that the apparent viscosity measurement could determine the difference in the material flow state in the out-of-plane direction due to the presence or absence of the rib shape.

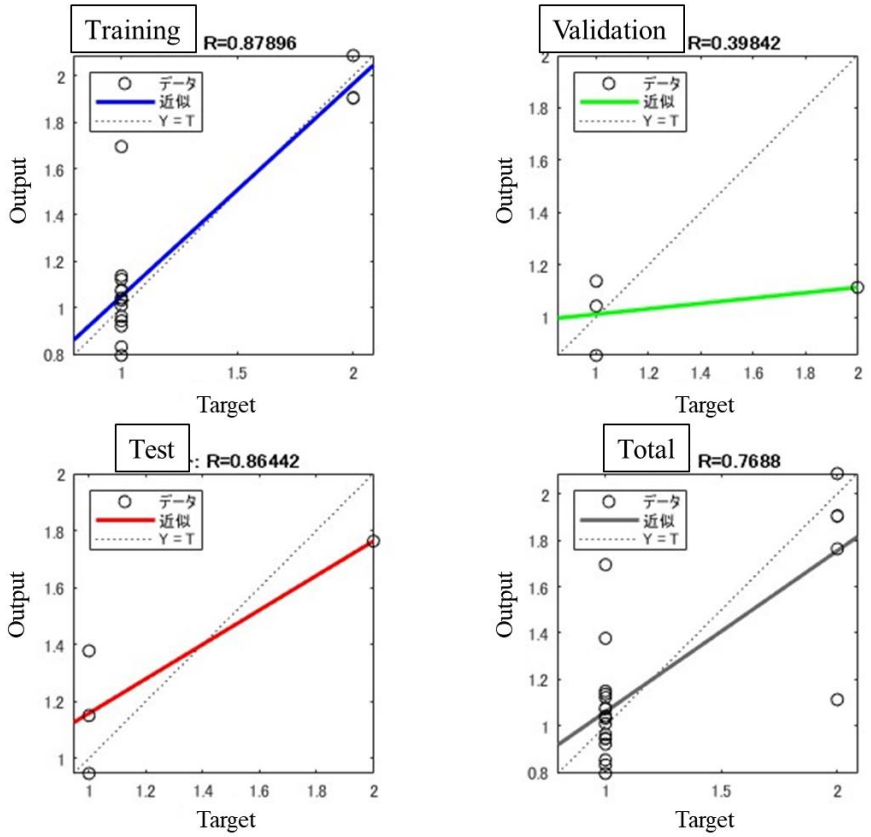

Fig. 3-9 the results of each training, validation, and test phase from MATLAB application.

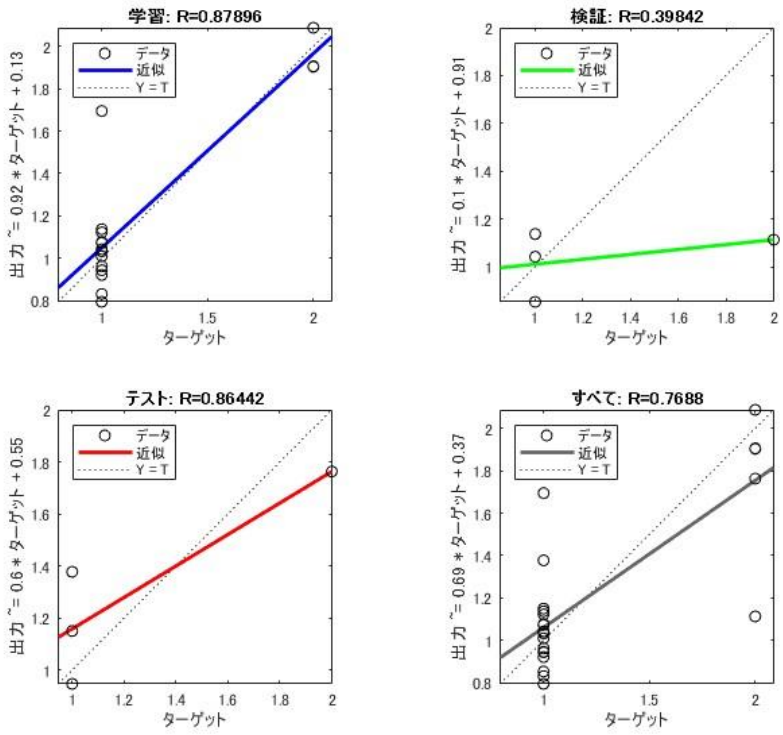

Fig. 3-10 The results of five times of learning from MATLAB application (1 times)

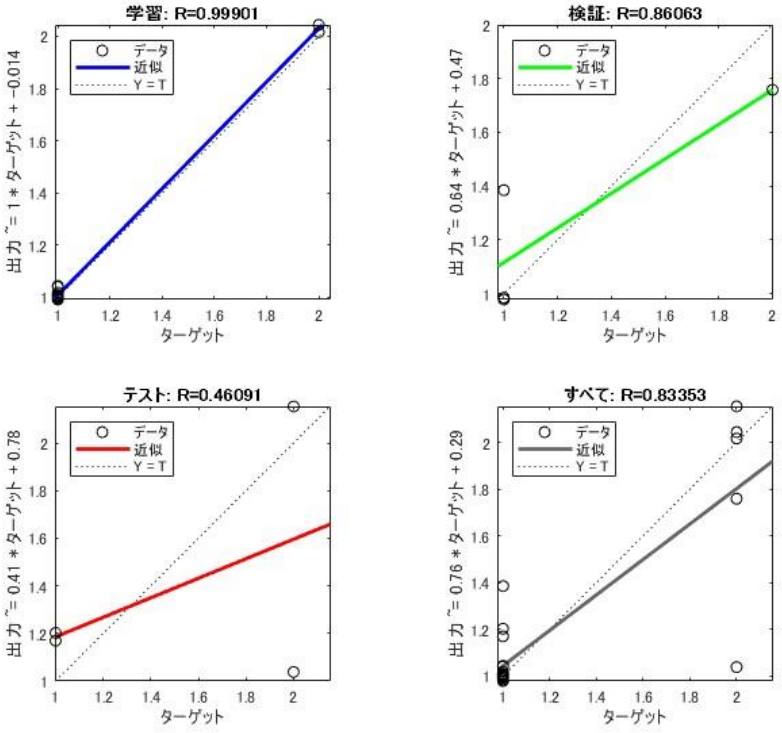

Fig. 3-11 The results of five times of learning from MATLAB application (2 times)

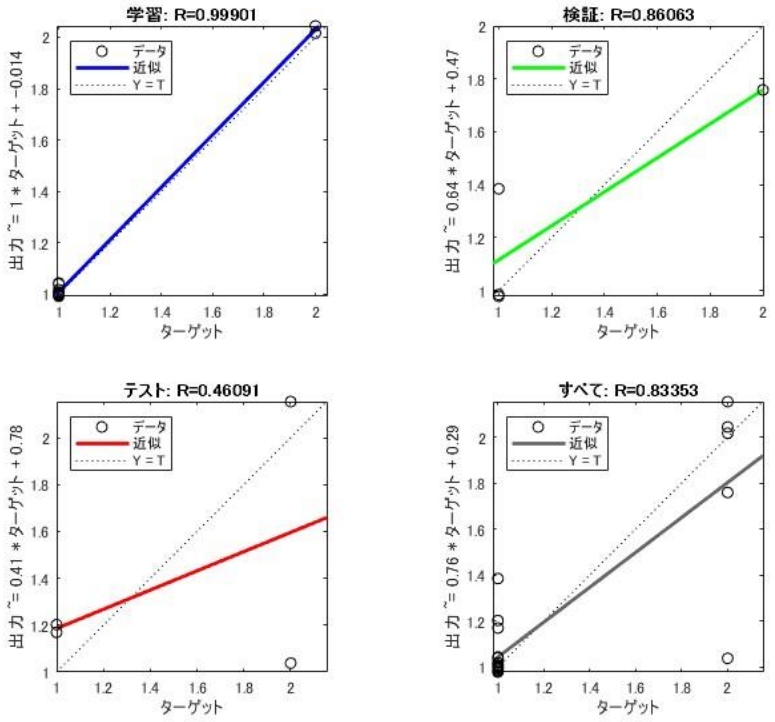

Fig. 3-12 The results of five times of learning from MATLAB application (3 times)

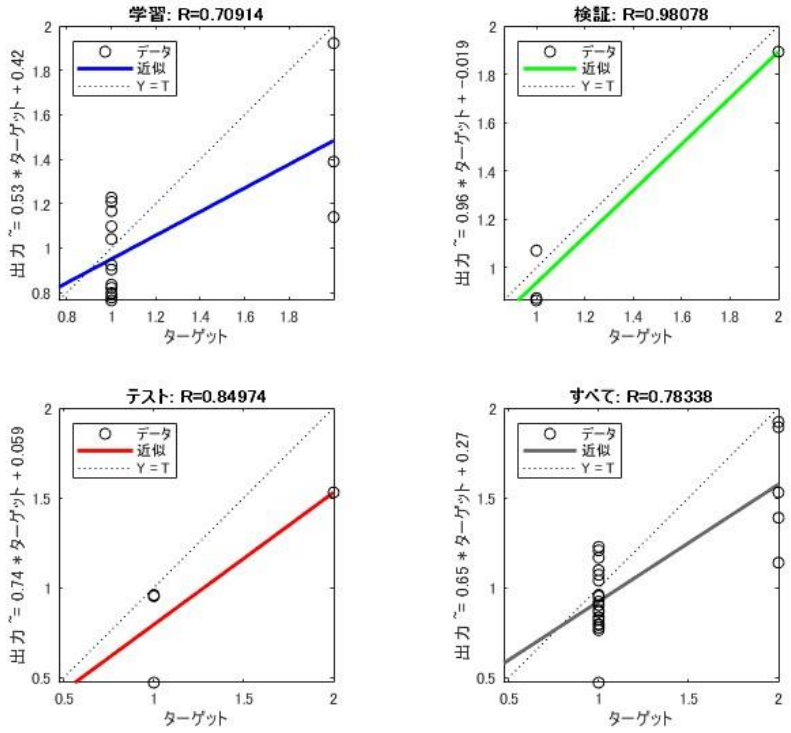

Fig. 3-13 The results of five times of learning from MATLAB application (4 times)

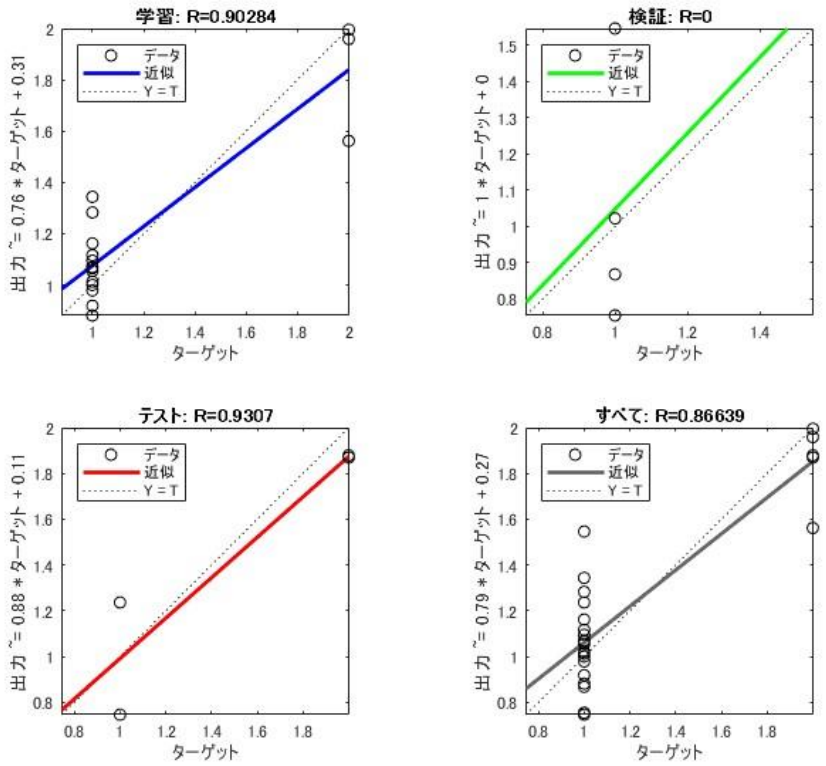

Fig. 3-14 The results of five times of learning from MATLAB application (5 times)

Table 3-1 the error R values resulting from Figures 3-10 to 3-14.

		Training	Validation	Test	Total
Train	1	0.88	0.40	0.86	0.77
	2	1.00	0.88	0.46	0.83
	3	1.00	0.86	0.46	0.83
	4	0.71	0.98	0.85	0.78
	5	0.90	0.00	0.93	0.87
Average		0.90	0.62	0.71	0.82

4. Conclusion

In Chapter 1, we could measure the material flow in the die during press molding, which a conventional sensor could not measure until now, by calculating the apparent viscosity by combined analysis with the die-mounted sensor. This study showed that the apparent viscosity indicates the flow of material during compressive load deformation. The material database obtained by measuring the universal material tester and the measured value of the press molding experiment was in good agreement.

In Chapter 2, The fiber orientation tensor of the molded product was obtained by the X-ray phase imaging, which is difficult to obtain by using the X-ray CT until now. The damage fracture prediction simulation, GENOA was used to calculate the physical properties of the laminated material from fiber orientation tensor data, and a damage failure simulation simulating a tensile test was performed. As a result of the above, when the anisotropic region was large in the test piece, the simulation fracture result and the actual test result were in good agreement. However, when the anisotropic region was small, the fracture positions of the simulation and the actual test did not always match. Focusing on the change in test piece strain immediately before fracture, the change in test piece structure under tensile load was a valid simulation result because there is a correlation between the simulation and the actual test result.

In Chapter 3, the flow condition of the material inside the mold was determined using the apparent viscosity. Using a molded product rib and ribless that simulates the defective state of short-shot molding, the MATLAB application's machine learning "Fit Data with a Shallow Neural Network" learned the apparent viscosity data during molding. Through machine learning, we were able to recognize differences in material flow conditions, which greatly affect the quality of molded products. With this technology, it is possible to make quality judgments based on sensor measurement data during press molding.

Summarizing the two years of this research, we have developed and demonstrated a technology that can accurately measure the material flow state in the mold during press molding, which was impossible until now, by calculating the apparent viscosity from sensor measurement data. We also demonstrated that machine learning can be used to determine the material flow state in the mold from the apparent viscosity, and we were able to achieve one of the purposes of this research.
Since the fiber orientation of the fiber composite material molding is closely related to the mechanical properties, a technology to measure the fiber orientation accurately is important. This research used a new X-ray phase imaging device to construct a fiber orientation analysis technology. Another objective of this study was to clarify the relationship between fiber orientation and apparent viscosity data to predict mechanical properties. However, 3D fiber orientation analysis of rib shape was very difficult and could not be achieved.

Reference

[1] S.F. Shuler, S.G. Advani, “Transverse squeeze flow of concentrated aligned fiber in viscous fluids”, J. Non-Newtonian Fluid Mech., 65, 47-74 (1996)

[2] P. Dumont, L. Orgras, D. Favire, P. Pizette, C. Venet, “Composite moulding of SMC: In situ experiments, modelling and simulation” Composites; Part A 38, 353-368 (2007)

[3] M. A, Dweib, C. M. O Bradaigh, “Extensional and shearing flow of a glass-mat-reinforced thermoplastics (GMT) material as a non-Newtonian viscous fluid”, Composites Science and Technology, 59, 1399-1410 (1999)

[4] R. P. Chhabra, “Rheology of Complex Fluids”, p.7 (2010), Springer Nature.

[5] H. Chun, J. Shin, I. M. Daniel, “Effects of material and geometric nonlinearities on the tensile and compressive behavior of composite materials with fiber waviness”, Composites Science and Technology 61 (2001)

[6] N. Morimoto, K. Kimura, T. Shirai, T. Doki, S. Sano, A. Horiba, and K. Kitamura, “Talbot–Lau interferometry-based x-ray imaging system with retractable and rotatable gratings for nondestructive testing”, Rev. Sci. Instrum. 91, 023706 (2020)

[7] F. Schaff, A. Malecki, G. Potdevin, E. Eggl, P. B. Noël, T. Baum, E. G. Garcia, J. S. Bauer and F. Pfeiffer,"Correlation of X-Ray Vector Radiography to Bone Micro-Architecture",Sci. Rep. 4, 3695(2014)

[8] Brian J. Jellison, Aaron S. Field, Joshua Medow, Mariana Lazar, M. Shariar Salamat, and Andrew L. Alexander,"Diffusion Tensor Imaging of Cerebral White Matter: A Pictorial Review of Physics, Fiber Tract Anatomy, and Tumor Imaging Patterns",AJNR Am J Neuroradiol 25:356–369, March 2004

[9] Tandon, G. P. and Weng, G. J, “The effect of aspect ratio of inclusions on the elastic propertied of un-directionally aligned composites”, Polymer Composites,5(4),327-333.

[10] M. Garg, F. Abdi, and J. Housner, ” Prediction of effect of waviness, interfacial bonding and agglomeration of carbon nanotubes on their polymer composites”, SAMPE 2013, Long Beach, CA.

[11] S. DorMohammadi, F. Abdi, R. Mandapati, H. K. Baid, M. Lee, U. Gandhi, “Impact Crush Modeling of Chopped Fiber Reinforced Polymers”, Conference: American Society of Composites-30th Technical Conference, 2015.

[12] C. Godiness, S. DorMohammadi, F. Abdi, M. V. Montero, D. Huang, L. Minnetyan, “Damage tolerant composite design principles for aircraft components under static service loading using multi-scale progressive failure analysis”, Journal of Composite Materials 51(10), 2016.

[13] Qinglin Qi, Fei Tao, Ying Zuo, Dongming Zhao, “Digital Twin Service towards Smart Manufacturing”, Procedia CIRP, Vol. 72, 2018.

[14] Qinglin Qi, Fei Tao, “Digital Twin and Big Data Towards Smart Manufacturing and Industry 4.0: 360 Degree Comparison”, IEEE Access, Vol. 6, 2018.

List of Conference presentation and Publications in 2020-2022

1. T. Shirai, M. Sakaguchi, K. Uzawa, K. Kimura, T. Doki, N. Morimoto, K. Shomei, "Examination of fiber orientation analysis by X-ray phase imaging and damage analysis using orientation data of the discontinuous carbon fiber random orientation laminate sheet", *Proceedings of Japan Composite C*onference Meeting 12 (JCCM12), 2021.
2. T. Shirai, K. Uzawa, "Control of material flow characteristics in rib molding dies by press molding conditions of the discontinuous tape randomly oriented thermoplastic CFRP", *Proceedings of Japan Symposium of Composite Meeting 46 (JCSM46),* 2021.
3. T. Shirai, K. Uzawa., "Study of melt viscosity of discontinuous fiber thermoplastic CFRP during press molding", *Proceedings of 17th Japan International SAMPE Symposium and Exhibition (JISSE17)*, 2021. (Schedule)
4. G. Cai, T. Shirai, Y. Wan, K. Uzawa, J. Takahashi, "Application of X-ray Computed Tomography to Measuring Fiber Orientation Distribution of Chopped Carbon Fiber Tape Reinforced Thermoplastics.", *Applied Composite Materials*, 28, 573–586 (2021).
5. T. Shirai, K. Uzawa, "Examination of material flow measurement method during press molding of discontinuous fiber random orientation thermoplastic CFRP", *Reinforced Plastic*, 2021.
6. T. Shirai, M. Sakaguchi, K. Uzawa, T. Doki, N. Morimoto, K. Kimura, K. Shomei, "Examination of fiber orientation analysis and damage fracture prediction simulation by X-ray phase imaging method for discontinuous carbon fiber random laminated molded products", *Japan Society for Composite Materials*, 2021. (Schedule).
7. T. Shirai, K. Uzawa, "Mechanical Characterization of Randomly Oriented Patterned CTT Using Automatic Tape Lamination Robot", Materials System, Vol. 40, 2023
8. T. Shirai, K. Uzawa, "Mechanical property control by orientation distribution design of cut tape random CFRTP using the automatic laminating robot.", *Proceedings of Japan Composite C*onference Meeting 14 (JCCM14), 2023.